Notch activity permits retinal cells to progress through multiple progenitor states and acquire a stem cell property

Ashutosh P. Jadhav*, Seo-Hee Cho†, and Constance L. Cepko†‡

*Harvard–Massachusetts Institute of Technology Division of Health Sciences and Technology and †Department of Genetics and Howard Hughes Medical Institute, Harvard Medical School, 77 Avenue Louis Pasteur, Boston, MA 02115

Contributed by Constance L. Cepko, October 10, 2006 (sent for review November 9, 2005)

Signaling through the Notch pathway regulates multiple aspects of development. The vertebrate retina allows an investigation of the basis for these various effects, because the major cell types of the retina arise from a common progenitor that expresses *Notch1*. The Notch pathway was constitutively activated in distinct populations of retinal cells during development. Prolonged Notch activity in progenitor cells maintained cells in the progenitor state without perturbing temporal identity, promoting early progenitor characteristics early in development and late progenitor characteristics later in development. Eventually, constitutive Notch activation led these cells to acquire characteristics of glial and stem cells. In contrast, reactivating the Notch pathway in newly postmitotic retinal cells promoted mature glial cell formation in a subset of cells. These data suggest that prolonged Notch activity does not disrupt the normal progression of progenitor temporal states, and that down-regulating or overcoming Notch activity is required for proper formation of both neuronal and glial cell fates.

development | glia | retina

The generation of cellular diversity during development requires that progenitor cells dynamically interpret both intrinsic and extrinsic cues (1, 2). Notch is a transmembrane receptor that transduces an extrinsic cue, that of the binding of its ligand, e.g., Delta or Serrate, to directly activate transcription of as-yet ill-defined target genes (3). Studies in both the vertebrate and invertebrate nervous systems have established a critical role for Notch signaling in preserving a pool of undifferentiated progenitor cells (3). More recent studies have suggested an additional role for activated Notch in specifying or promoting a particular cell fate, the glial cell fate (4–6). Furthermore, Notch activity also has been shown to induce stem cell features and participate in neuronal subtype specification (7–9). These studies raise the question of how Notch activity can influence the generation of multiple cell fates, while also acting in a more generic fashion to preserve a progenitor pool.

The vertebrate retina is a paradigm for studying the mechanisms of cell fate determination (1, 10, 11). All major cell types are known to arise sequentially in a conserved order from multipotent progenitors. Studies in frog, rat, chick, and mouse have shown that *Notch1* is expressed by proliferating and undifferentiated cells during development (12–14). Among the last cells generated in the retina are Müller glial cells, which retain expression of *Notch1* (4, 12). Constitutive activation of the Notch pathway by overexpression of the intracellular domain of Notch (NIC) in fish, frog, chick and rat retina has been shown to inhibit neurogenesis (12, 13, 15, 16). Furthermore, NIC-overexpressing cells in the fish and rat acquire glial features (4, 16), suggesting that Notch may instruct gliogenesis at the expense of neuronal production. In contrast, activation of the Notch pathway in the early frog retina did not seem to promote gliogenesis but resulted in nondividing cells with neuroepithelial morphology (12). It is unclear whether these differences were due to the timing and/or dose of prolonged Notch activity.

Here, we show that activation of Notch in mitotic retinal progenitor cells allows the normal temporal progression of progenitor cells, leading eventually to cells that express features of glial cells, in keeping with previous results (4). However, a comprehensive molecular characterization revealed that these cells also express progenitor genes not expressed by normal Müller glia. A functional assay showed that these cells could form neurospheres, as can stem cells, whereas normal retinal cells were unable to form such spheres. In contrast, when Notch was activated in postmitotic cells, glial cells without progenitor or stem cell features were produced.

Results

Constitutive Notch Activity in Embryonic Progenitor Cells Promotes Formation of Cells with Glial and Progenitor Features in the Postnatal Retina. To determine the role of Notch signaling in embryonic mouse retinal development, the Notch pathway was constitutively activated by crossing $Rosa^{N1\text{-}IC}$ (17) mice to mice expressing Cre recombinase under the *Chx10* promoter (*Chx10-CRE*; ref. 18). The $Rosa^{N1\text{-}IC}$ mice contain, in the ubiquitously expressed *Rosa26* locus, a STOP sequence flanked by loxP sites followed by an NIC (Fig. 6*A*, which is published as supporting information on the PNAS web site). Upon exposure to Cre recombinase, the STOP sequence is removed, and NIC is expressed. In addition, an internal ribosomal entry sequence and the gene for nuclear-localized enhanced GFP leads to GFP expression. This allows for expression of NIC and nuclear GFP in Cre+ cells and their descendants. Expression of Cre in *Chx10-CRE* mice begins at embryonic day (E)11–E12 in retinal progenitor cells and is relatively specific to the retina (18).

The eventual fate of NIC-expressing progenitor cells was assayed at postnatal day 10 (P10), when development is nearly complete. The retinae from NIC-overexpressing mice (*Chx10-CRE*/+; $Rosa^{N1\text{-}IC}$/+ or $Chx10^{N1\text{-}IC}$) were folded and smaller (Fig. 6*C*) relative to WT retinae (Fig. 6*B*). Cryosections revealed that the $Chx10^{N1\text{-}IC}$ retina had a slightly smaller outer nuclear layer, expanded inner nuclear layer (INL), and reduced inner plexiform layer, causing the ganglion cell layer to compress against the INL (compare Fig. 1 *E* and *F*). RNA *in situ* hybridization (ISH) was performed on $Chx10^{N1\text{-}IC}$ vs. WT retinae for *Notch1*, *Delta1* (*Dll1*), *Hes1*, and *Hey1*. At this stage, expression of *Notch1* and *Hes1* is localized to Müller glia, *Hey1* is localized to progenitors (4, 19), and *Delta1* ISH signal is no longer detectable (13). In $Chx10^{N1\text{-}IC}$ mice, *Notch1* itself was up-regulated (Fig. 1 *A* vs. *B*), as were its canonical targets, *Hes1* and *Hey1*, whereas *Dll1* was unchanged (data not

Author contributions: A.P.J. and C.L.C. designed research; A.P.J. and S.-H.C. performed research; A.P.J. contributed new reagents/analytic tools; A.P.J., S.-H.C., and C.L.C. analyzed data; and A.P.J. and C.L.C. wrote the paper.

The authors declare no conflict of interest.

Freely available online through the PNAS open access option.

Abbreviations: ISH, *in situ* hybridization; INL, inner nuclear layer; NIC, intracellular domain of Notch; P*n*, postnatal day *n*; E*n*, embryonic day *n*.

†To whom correspondence should be addressed. E-mail: cepko@genetics.med.harvard.edu.

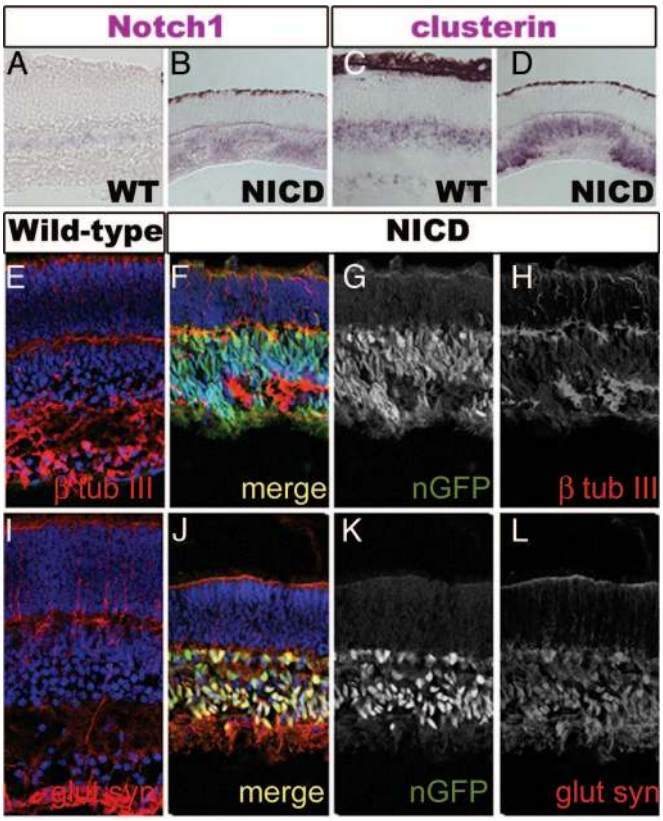

Fig. 1. Directed misexpression of NIC in *Chxlo* expression cells. Section ISH on WT (*A* and *C*) and *Chx10*$^{N1\text{-}IC}$ (*B* and *D*) retinae at P10. (*A* and *B*) *Notch1*. (*C* and *D*) *clusterin*. Immunostaining on WT (*E* and *I*) and *Chx10*$^{N1\text{-}IC}$ (*F–H* and *J–L*) retinae at P10. (*E* and *F*) Merge of DAPI, nGFP, and β tubulin III (β tub III). (*I* and *J*) merge of DAPI, nGFP, and glutamine synthetase (glut syn). (*G* and *K*) nGFP. (*H*) β tubulin III. (*L*) glut syn.

shown). The *Notch1* RNA ISH probe used does not recognize NIC, and thus this up-regulation reflects endogenous *Notch1* expression.

Previously, it was shown that misexpression of NIC in rat P0 retinal progenitor cells promoted glial features and inhibited neuronal cell fates (4, 13). To determine whether a similar phenotype resulted in the *Chx10*$^{N1\text{-}IC}$ retina, immunostaining was performed for the neuronal antigen, β tubulin III, and the glial marker, glutamine synthetase. Because NIC-overexpressing cells coexpress nuclear GFP, cells expressing NIC could be visualized. The GFP+ cells localized strictly to the INL/ganglion cell layer, and these cells did not exhibit β tubulin III immunoreactivity (Fig. 1*F*) but did express glutamine synthetase (Fig. 1*J*). Furthermore, RNA ISH for a mature glial cell marker, *clusterin* (20), also revealed an increase of this transcript (Fig. 1 *C* vs. *D*).

Progenitor Features Persist in Retinal Cells Expressing NIC. RNA was isolated from a single WT or *Chx10*$^{N1\text{-}IC}$ retina at P10, and gene expression was assayed in duplicate on microarrays. Genes with a ratio of WT vs. mutant intensity <1 (Table 1), and >1 in the *Chx10*$^{N1\text{-}IC}$ retinae were found (Table 2).

The signals from multiple neuronal genes were lower in the *Chx10*$^{N1\text{-}IC}$ retinae, including *cone blue opsin*, *L7*, *calbindin 2*, and *neurofilament light polypeptide* (Table 2). ISH for the rod photoreceptor-specific marker, *NRL*, and the cone photoreceptor marker, *blue cone opsin*, confirmed they had a lower expression than the control (data not shown). The signals that were higher in the *Chx10*$^{N1\text{-}IC}$ retinae included those for known glial markers, such as *carbonic anhydrase 2* and *retinaldehyde binding protein 1* (20, 21). These results suggest that Notch activity promotes glial cell fate. However, progenitor genes, such as *fibroblast growth factor 15* (*FGF15*) and *cyclin D1* (20, 22), also had higher signals in the *Chx10*$^{N1\text{-}IC}$ retinae (Table 1).

To confirm these profiling results, ISH was performed for *FGF15* and *cyclin D1*. Both of these genes are weakly or not expressed at P10, when much of development is complete (20), but were expressed in the NIC-expressing retinae (Fig. 2*A–D*). Furthermore, WT and *Chx10*$^{N1\text{-}IC}$ retinae were immunostained for Pax6 and Chx10. At this age, anti-Pax6 antibody marks amacrine, ganglion, and horizontal cells, anti-Chx10 marks bipolar cells and, very weakly, a minority of Müller glia. During development, both of these genes are expressed in most, if not all, retinal progenitor cells (18, 23). In the WT retina, Pax6 expression can be detected in the lower half of the INL and ganglion cell layer (Fig. 2*E*), consistent with expression in amacrine and ganglion cells. Interestingly in the *Chx10*$^{N1\text{-}IC}$ retinae, Pax6 was expressed at a high level throughout the INL and found to be colocalized with the GFP-positive cells (Fig. 2*F*). Chx10 was also found to be expressed at a higher level and colocalized with the NIC-expressing cells (data not shown).

Notch Activity Promotes Early Progenitor but Not Late Progenitor or Glial Features in the Embryonic Retina. It was of interest to determine whether Notch activity was sufficient for precocious expression of late progenitor and/or glial genes in early progenitor cells, which normally do not express them. Gene expression profiling was performed on the E13.5 WT and *Chx10*$^{N1\text{-}IC}$ retinae. RNA was isolated from retinae pooled from two WT or mutant mice, and the experiment was performed as a color-swap duplicate. Many of the genes with lower signals in the Chx10$^{N1\text{-}IC}$ retinae are markers of retinal ganglion cells, such as *GAP43* and *neurofilament light polypeptide* (*NF-L*). Because this is the major neuronal cell type present at this age, neurogenesis is most likely inhibited in the NIC-overexpressing cells. Genes with higher signals in the *Chx10*$^{N1\text{-}IC}$ retinae included *Notch1*; known Notch targets, such as *Nrarp* (24); and progenitor genes, such as *Chx10*, *FGF15*, and *Sox9* (Table 3; ref. 20). *Hey1* appeared to have both higher (Table 7) and lower (Table 6) signals by gene expression profiling, for reasons that are unclear. However, section ISH showed that *Hey1* levels were higher in the *Chx10*$^{N1\text{-}IC}$ retinae relative to the WT retinae (data not shown). Section ISH also confirmed that expression of both *Notch1* and *FGF15* was in a higher number of cells in the *Chx10*$^{N1\text{-}IC}$ retinae at E13.5 (Fig. 3 *A*, *B*, *F*, and *G*). The mature glial gene, *clusterin*, and the late progenitor/glial marker, *mu crystallin*, were not expressed at a higher level by gene profiling or by RNA ISH (Fig. 3 *E* and *J* and data not shown) in the *Chx10*$^{N1\text{-}IC}$ retinae at this early age.

The expression of several genes was higher in the E13.5 *Chx10*$^{N1\text{-}IC}$ retinae but not in the P10 *Chx10*$^{N1\text{-}IC}$ retinae. One of these genes is *secreted frizzled-related protein 2* (*Sfrp2*), a marker of early retinal progenitor cells (20). A screen of the uncharacterized genes expressed at a higher level in *Chx10*$^{N1\text{-}IC}$ retinae revealed that several are expressed in early retinal progenitor cells, but not in late retinal progenitor cells in the WT retina (data not shown). One of these novel markers is *deiodonase 3 anti-sense* (*Dio3as*), which, like *Sfrp2*, is expressed robustly in normal retinal progenitor cells at E13 and E14, weaker at E16.5, and only visible in the peripheral retina by P0 (Fig. 7, which is published as supporting information on the PNAS web site). Analysis of *Sfrp2* and *Dio3as* expression in the *Chx10*$^{N1\text{-}IC}$ retinae by ISH revealed that expression of both of these genes was in a higher number of cells in the NIC-overexpressing retinae at E13.5 (Fig. 3 *C*, *D*, *H*, and *I*) but not at P10 (data not shown).

There was no apparent increase in retinal size at early (E13.5 and E16.5) and late time points (P0 and P10), as might be expected with an increased number of progenitor cells. To examine whether cells may have been eliminated by apoptosis, TUNEL staining was performed on WT and Chx10$^{N1\text{-}IC}$ retinae at E14.5 and P0, P4, and P10. No differences in TUNEL labeling were observed (data not shown). To further examine the influence of NIC overexpression on

Table 1. Genes with higher expression in NIC-expressing retinal cells relative to WT cells at P10

GenBank no.	Symbol	Unigene	Gene name	Exp1-UP	Exp2-UP	Average
—	GFP	—	GFP	5.59	5.88	5.73
BE952015	Fgf15	Mm.3904	Fibroblast growth factor 15	4.72	2.97	3.84
AI838192	Dkk3	Mm.55143	Dickkopf homolog 3 (*Xenopus laevis*)	4.28	2.34	3.31
BE949664	H19	Mm.350055	H19 fetal liver mRNA	3.78	2.69	3.23
BF464158	Cdkn1c	Mm.168789	Cyclin-dependent kinase inhibitor 1C (P57)	2.74	3.21	2.98
BF465231	Rlbp1	Mm.41653	Retinaldehyde binding protein 1	3.55	2.17	2.86
BE995092	Nrarp	Mm.46539	Notch-regulated ankyrin repeat protein	3.26	2.23	2.75
AI851652	Hey1	Mm.29581	Hairy/enhancer-of-split related with YRPW motif 1	3.38	2.11	2.74
—	Ccnd1	Mm.273049	Cyclin D1	3.28	1.91	2.60
BE953342	Car2	Mm.1186	Carbonic anhydrase 2	2.88	1.98	2.43

proliferation in the early retina, E14.5 retinae were harvested from WT and $Chx10^{N1\text{-}IC}$ mice and pulsed with BrdU for 1 h. Retinae were dissociated and then immunostained with anti-BrdU. The percentage of DAPI-positive cells that incorporated BrdU was 19% +/− 1% in the WT retinae as compared with 20% +/− 3% in the $Chx10^{N1\text{-}IC}$ retinae.

Late Retinal Progenitor Cells Acquire a Stem Cell Feature in Response to Constitutive Notch Activity. The above results suggest that retinal progenitor cells respond to Notch activity by sustaining a progenitor program that is temporally appropriate. Cells with stem cell characteristics have been reported to reside in the pigmented ciliary margin of adult mouse, rat, and human retinae (25, 26). *In vitro*, these cells form pigmented neurospheres, self-renew, and are multipotent. Interestingly, the frequency of neurosphere-forming cells was found to be greater in the mouse retina at the adult stage, compared with E14.5 (25), suggesting that the number of stem cells increases with developmental time.

To assay the NIC-overexpressing cells for stem cell features, the central portions of WT (Fig. 4*A*) and $Chx10^{N1\text{-}IC}$ retinae (Fig. 4*D*) were dissociated and cultured *in vitro* by using a neurosphere assay. The level of GFP expression was assessed on three additional retinae by using GFP immunohistochemistry and confocal microscopy, which showed that an average of 26.9% of the total population expressed GFP. Cells from $Chx10^{N1\text{-}IC}$ retinae aged P21–P25 (n = 22) were cultured in the presence of EGF and basic FGF (FGF2; Fig. 4 *E–F*). They gave rise to 3–78 spheres per retina, with an average of 32 +/−23.9 (SD) spheres. In cultures from two different mice, some of the spheres were composed of darkly pigmented and nonpigmented cells (Fig. 4 *E–F*). All spheres obtained from $Chx10^{N1\text{-}IC}$ retinae contained GFP+ cells (Fig. 4 *G–I*). To compare the sphere-forming frequency of central retinal cells to that obtained with cells from the ciliary margin, cells were cultured from the ciliary margin of the $Chx10^{N1\text{-}IC}$ retinae (n = 8). An average of 9.9 +/−8.4 (SD) spheres was observed, whereas an average of 11.5 +/−12.7 (SD) were formed from the ciliary margin of the WT retinae (n = 8). To determine whether primary spheres from $Chx10^{N1\text{-}IC}$ retinae had extended proliferative capacity, cells were dissociated and passaged. Approximately 9% of the primary neurospheres could form secondary spheres, and of these, ≈10% could form small tertiary neurospheres. In contrast to the sphere-forming capacity of cells from $Chx10^{N1\text{-}IC}$ retinae, no spheres were observed to derive from WT retinae (n = 20, Fig. 4 *B* and *C*). In keeping with this observation, no GFP-negative spheres were obtained from $Chx10^{N1\text{-}IC}$ retinae.

To determine whether neurosphere-forming capacity extended to later periods, cells from P60 $Chx10^{N1\text{-}IC}$ retinae were assayed (n = 6). Spheres were observed, with an average of 48.8 +/−35 (SD) neurospheres and a range of 7–88 per retina. The GFP immunohistochemistry of older retinae showed 19.7% of the cells expressed GFP, and spheres derived from this age had GFP+ cells.

Reactivation of the Notch Pathway in Postmitotic Retinal Cells Induces Formation of Müller Glia. Although Notch activation in early retinal progenitor cells promoted glial features in late retinal progenitor cells, proper glial formation most likely did not occur, because these cells exhibited progenitor and stem cell features not normally found in glia. Similarly, we reported previously that the morphology of NIC-expressing late cells was not that of normal Müller glia (4). These findings suggest that all mature cell types of the retina, including glia, require release from Notch activity to properly differentiate. It is possible that Müller glial cells arise from a proliferating progenitor that down-regulates its Notch activity, exits the cell cycle, and then reactivates the Notch pathway to promote glial fate. To test this model, Notch activity was reactivated in a newly postmitotic population of cells, by breeding $Rosa^{N1\text{-}IC}$ mice to mice expressing Cre recombinase under the *Sonic hedgehog* (*Shh*) promoter (Fig. 5*A*; ref. 27).

Shh is known to be expressed in retinal ganglion cells in the mature mouse retina (28). When *Shh-CRE* mice were crossed to the conditional *Rosa26R* mice (29), lacZ staining could be observed in amacrine cells and cone photoreceptor cells, in addition to ganglion cells (Fig. 5*B*). Lineage analysis has demonstrated that most clones derived from embryonic retinal progenitor cells containing more than two cells include at least one rod photoreceptor (30). Because Shh descendants do not include rod photoreceptors, *Shh* expression is most likely excluded from retinal progenitor cells but is in a

Table 2. Genes with lower expression in NIC-expressing retinal cells relative to WT cells at P10

GenBank no.	Symbol	Unigene	Gene name	Exp1-DOWN	Exp2-DOWN	Average
—	Opn1sw	Mm.56987	Opsin 1 (cone pigments), short-wave-sensitive	0.12	0.19	0.16
BE981218	Pde6h	Mm.290622	Phosphodiesterase 6H, cGMP-specific, cone, gamma	0.12	0.27	0.20
AI843793	Pcp2	Mm.254898	Purkinje cell protein 2 (L7)	0.16	0.26	0.20
BE954739	Guca1a	Mm.16224	Guanylate cyclase activator 1a (retina)	0.16	0.29	0.22
AI835609	Nefl	Mm.1956	Neurofilament, light polypeptide	0.19	0.31	0.25
BE950544	Gnal2	Mm.374791	Guanine nucleotide-binding protein, α transducing 2	0.22	0.32	0.27
BE954252	Calb2	Mm.2755	Calbindin 2	0.19	0.41	0.30
—	Opn1mw	Mm.284825	Opsin 1 (cone pigments), medium-wave-sensitive	0.16	0.44	0.30
BE951286	Isl1	Mm.42242	ISL1 transcription factor, LIM/homeodomain (islet 1)	0.25	0.37	0.31
BF466274	Kcne2	Mm.156736	Potassium voltage-gated channel, Isk-related subfamily, gene 2	0.27	0.38	0.32

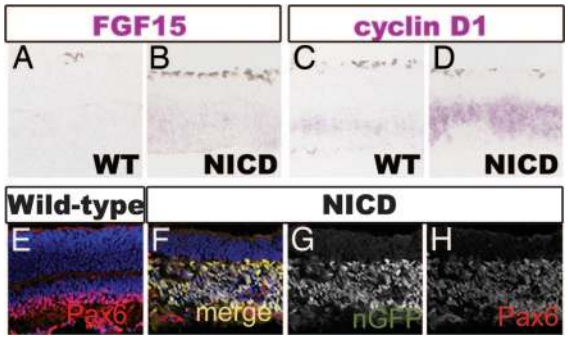

Fig. 2. Gene expression changes in activated Notch retinal progenitor cells at P10. Section ISH on WT (*A* and *C*) and $Chx10^{N1\text{-}IC}$ (*B* and *D*) retinae at P10. (*A* and *B*) *FGF15*. (*C* and *D*) *cyclin D1*. (*E–H*) Immunostaining on WT (*E*) and $Chx10^{N1\text{-}IC}$ retinae with anti-Pax6 antibody at P10 (*F–H*). (*E–H*) Merge of DAPI, GFP, and Pax6 (*E* and *F*), nGFP (*G*), and Pax6 (*H*).

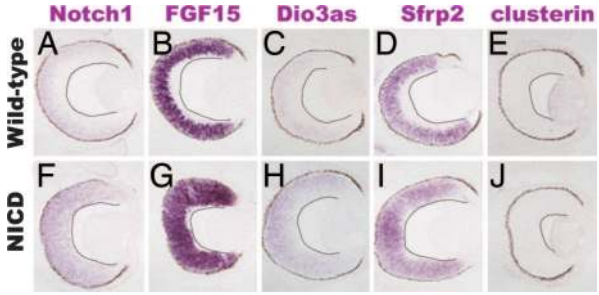

Fig. 3. Gene expression changes in activated Notch retinal progenitor cells at E13.5. Fold changes are averaged from a color-swap experiment. (*A–J*) Section ISH on WT (*A–E*) and $Chx10^{N1\text{-}IC}$ (*F–J*) retinae at E13.5. (*A* and F) *Notch1*. (*B* and *G*) *FGF15*. (*C* and *H*) *Dio3as*. (*D* and *I*) *Sfrp2*. (*E* and *J*) *clusterin*. A black line is drawn to indicate the vitreal edge of the retina.

population of postmitotic retinal cells that become cones, amacrine cells, and ganglion cells.

By crossing *Shh-CRE*/+; *R26R*/+ mice to $Rosa^{N1\text{-}IC}$/+ mice, NIC-overexpressing mice (*Shh-CRE*/+; $Rosa^{N1\text{-}IC}$/+ or $Shh^{N1\text{-}IC}$) were generated with the *Rosa26R* allele. Gross examination of the retinae from these mice at P11 revealed no apparent size difference from WT retinae. GFP was difficult to visualize in these retinae on whole-mount or on sections possibly due to low promoter activity in these cells, and so β-gal activity was used to analyze these cells. X-Gal staining in the retinae at P11 revealed a pattern markedly different from the one observed in the *Shh-CRE*/+; *R26R*/+ retinae. There was strong X-Gal staining in the INL, in addition to diffuse staining in the outer nuclear layer, consistent with scleral Müller glial cell processes (Fig. 5*C*). To better characterize the NIC-overexpressing cells, $Shh^{N1\text{-}IC}$ with the *Rosa26R* allele were immunostained for β-gal, glutamine synthetase (a Müller glial cell marker), and Pax6 (a marker of retinal progenitor, retinal ganglion, horizontal, and amacrine cells). Visualization of the β-gal+ cells by confocal microscopy revealed that many of these cells coexpressed glutamine synthetase (Fig. 5 *D–F*). This suggests that at least a subset of NIC-overexpressing cells acquired glial cell characteristics. Interestingly, staining for Pax6 revealed a WT distribution of expression, with cells in the lower part of the INL and in the ganglion cell layer (Fig. 5*H*). Only a subset of the β-gal+ cells in the INL and ganglion cell layer expressed Pax6 (Fig. 5*I*). These results demonstrate that at least a subset of NIC-expressing cells express Pax6 and exhibit a morphology consistent with being amacrine and ganglion cells. Importantly, many of the β-gal+ cells that expressed glutamine synthetase were located above the Pax6-expressing layer of the INL, in the position of normal Müller glia. In contrast to the $Chx10^{N1\text{-}IC}$ retinae, central retina from adult $Shh^{N1\text{-}IC}$ did not give rise to neurospheres when dissociated and cultured in the presence of EGF and FGF2 factor ($n = 5$).

Discussion

Activation of Notch in early progenitor cells allowed them to retain appropriate early progenitor gene expression. These cells did not precociously express glial markers or late progenitor genes at early stages of development. When examined at later stages of development, however, the cells exhibited expression of an inappropriate mixture of late progenitor and glial genes. When such cells were taken from the adult retina and cultured in EGF/FGF2, neurospheres were formed, as is observed with normal retinal stem cells taken from the retinal periphery (25), or Müller glia cultured in certain conditions (31). In contrast, activation of the Notch pathway in newly postmitotic cells led to a subset of cells with glial gene expression and proper glial morphology, in the absence of progenitor or stem cell characteristics, suggesting that proper glial differentiation requires a release from Notch activation. These data, together with recent findings that Notch can inhibit the formation of photoreceptor cells (8, 9), support an iterative role for Notch in nervous system development. We propose that Notch signaling regulates the neuronal vs. glial fate choice, perhaps in the mitotic cell which is also using Notch signal to regulate the decision to produce a postmitotic daughter. A second point of action might be in a newly postmitotic cell where a cell fate decision is being further regulated, i.e., to be a photoreceptor cell vs. another neuronal cell type.

The observation that the progenitor progression occurs normally in NIC-expressing progenitor cells is in keeping with several other observations. Large, retrovirally marked clones in the murine or chick retina contain cell types that are born exclusively early and exclusively late in development, e.g., ganglion and Müller glia cells (31, 32). Such clones can arise only if an initially infected progenitor cell makes a postmitotic daughter(s) early and a progenitor daughter(s) that progresses to a late state of competence. We propose that low or absent Notch activity in some daughter cells leads them to exit, whereas high Notch activity permits daughter cells to remain proliferative and undifferentiated while simultaneously allowing

Table 3. Genes that had higher expression in $Chx10^{N1\text{-}IC}$ retinae relative to WT at E13.5

GenBank no.	Symbol	Unigene	Gene name	Exp1-UP	Exp2-UP	Average
—	GFP	—	GFP	12.06	9.76	10.91
BF466513	Fgf3	Mm.4947	FGF 3	2.10	1.82	1.96
AI851652	Hey1	Mm.29581	Hairy/enhancer-of-split related with YRPW motif 1	1.87	1.90	1.89
BF460710	Sox9	Mm.286407	SRY-box containing gene 9	1.90	1.88	1.89
BE995092	Nrarp	Mm.46539	Notch-regulated ankyrin repeat protein	1.69	2.03	1.86
BE952015	Fgf15	Mm.3904	FGF 15	1.78	1.91	1.84
AI851596	Sfrp2	Mm.19155	Secreted frizzled-related sequence protein 2	2.16	1.44	1.80
—	Idb1	Mm.444	Inhibitor of DNA binding 1	1.53	1.69	1.61
—	Chx10	Mm.4405	*Caenorhabditis elegans* ceh-10 homeodomain-containing homolog	1.71	1.51	1.61
BE951547	Dio3as	Mm.351717	Deiodinase, iodothyronine type III, antisense	1.43	1.72	1.57

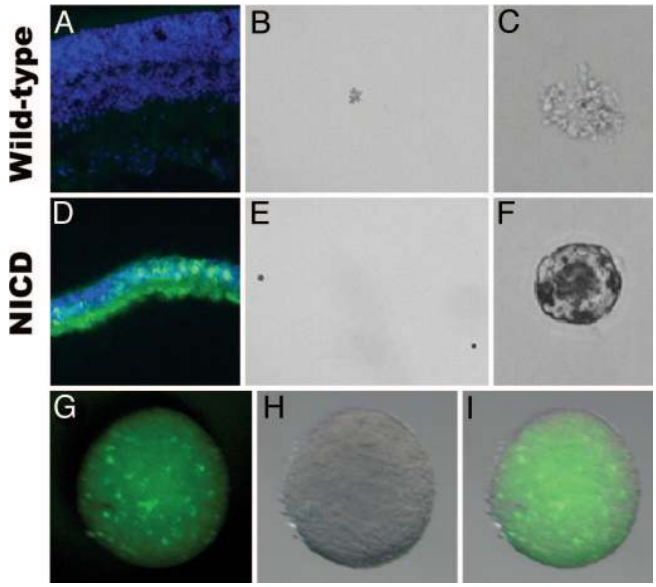

Fig. 4. Neurosphere assay of *Chx10*$^{N1\text{-}IC}$ retinal cells. Immunostaining and merge of DAPI and GFP on WT (*A*) and Chx10$^{N1\text{-}IC}$ (*D*) retinae at P21 is shown. Adult retinae from WT (*B* and *C*) and Chx10$^{N1\text{-}IC}$ (*E* and *F*) were dissociated and cultured in serum-free media with EGF and basic FGF *in vitro* and visualized by light microscopy at low (*B* and *E*) and high (*C* and *F*) magnification. (*G–I*) Spheres derived from Chx10$^{N1\text{-}IC}$ retinae contained GFP+ cells.

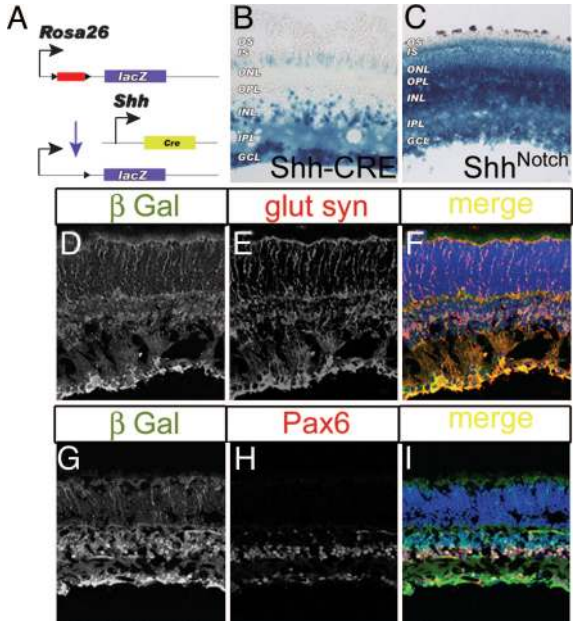

Fig. 5. Directed misexpression of NIC in *Shh*-expressing cells. (*A*) Diagram of transgenic constructs. The *Shh-CRE* mice have a CreGFP fusion under control of the *Shh* promoter (27). *Shh*$^{N1\text{-}IC}$ mice were generated by crossing the *Shh-CRE* allele into *Rosa*$^{N1\text{-}IC}$/*Rosa*$^{N1\text{-}IC}$ mice. Fate mapping of recombined cells was possible by additionally crossing these mice to *ROSA26-R* (*R26R*) mice. *R26R* is a Cre-recombinase reporter comprising a loxP flanked transcriptional STOP preceding a β-gal coding region (lacZ) (29). (*B* and *C*) X-Gal staining of P11 retinae from control (*B*) and *Shh*$^{N1\text{-}IC}$ (*C*) mice. (*D–I*) Immunostaining of *Shh*$^{N1\text{-}IC}$ retinae at P11. (*F*) Merge of DAPI, anti-β-galactosidase (β Gal), and anti-glutamine synthetase (glut syn). (*I*) merge of DAPI, anti-β-gal (β Gal), and anti-Pax6. (*D* and *G*) β Gal. (*E*) glut syn. (*H*) Pax 6. For control staining of WT retinae, see Figs. 1 (glutamine synthetase) and 2 (Pax6).

such progenitor daughters to pass through the stages of competence. Repeated or sustained Notch activity in some daughter cells within a single clone ultimately leads to large clones that contain both early- and late-born cell types. Furthermore, this aspect of Notch activity may be a general feature of nervous system development. Sustaining Notch activity for a period and then releasing it in the cerebral cortex allowed resumption of the production of the temporally appropriate neurons (33). Similarly, the well defined progenitor progression which occurs in the *Drosophila* CNS does not depend on the precise regulation of Notch activity (34).

It is interesting to note that hyperproliferation was not observed in the early NIC-expressing retinae. This implies that although proper Notch1 function is necessary for normal retinal size (8, 9) excess Notch activation is not sufficient to drive proliferation in the early retina, in keeping with observations of NIC introduction into early chick and *Xenopus* retinae (12, 15). In addition, it implies that the progenitor progression does not result from a precise regulation of neuron production, e.g., a counting of the number or types of neurons produced. It was possible that the progenitor progression depended upon feedback inhibition or feed-forward induction mediated by neurons produced by each competency state. Instead, we find that this progression appears to occur normally even in the absence of normal production of neurons, which is also in keeping with previous studies of *Xenopus* and murine retinal development (35). In the early *Xenopus* retina, all cell cycles were blocked with a DNA synthesis inhibitor, but all cell types formed (36), and in the *cyclin D1* mutant mouse retina, fewer cell cycles occurred, but the normal complement of retinal cells was made (refs. 22 and 37; C. Ma and C.L.C., unpublished observations). Furthermore, the data from other mutants, including *Math5*-null mice, where no ganglion cells are made and the *Pax6* conditional mutant, where only a subset of amacrine cells are made, also suggest that the progenitor progression occurs in the absence of differentiation cues produced by early-born neurons (38–40).

A subset of the late NIC-overexpressing cells can form primary neurospheres in a neurosphere colony forming assay, whereas normal retinal cells did not do so under our conditions. This demonstrates that the progression of NIC-expressing cells from an early- to a late-progenitor state terminates with glial and stem cell features. Adult retinal stem cells may be a specialized type of late-born Müller glial cell, lineally related to embryonic retinal progenitor cells. Some of these cells may become spatially restricted to the peripheral retina from which they can be cultured as neurospheres (17). In addition, Müller glia in the avian and mouse retina can proliferate and retain multipotency *in situ* in response to injury (41, 42), and a small fraction of murine cells can exhibit such properties after a culture period (31).

Together, these observations suggest that the cooperation of peripheral signals (e.g., Wnt2b; refs. 43 and 44), along with intrinsic signaling (e.g., high Notch activity), may ultimately regulate the stem cell potential of retinal cells. A similar lineage relationship between embryonic progenitors, glial, and stem cells has been proposed for other areas of the forebrain (45). This is best supported by the finding that periventricular astrocytes are adult neural stem cells, and that radial glial cells can give rise to all of the terminally differentiated cell types of the brain (i.e., neurons, astrocytes, oligodendrocytes, and ependymal cells) and adult neural stem cells (46, 47). Lineage studies tracing the clonal relationships among the six neuronal cell types, Müller glial cells, and adult retinal stem cells will definitively establish whether adult retinal stem cells are derived from retinal progenitor cells at the end of development.

Materials and Methods

Animals. Mice carrying the *Chx10-CRE BAC* transgene (18) or *Rosa*$^{N1\text{-}IC}$ allele (17) were crossed to generate mice hemizygous for *Chx10-CRE* and hemizygous for the *Rosa*$^{N1\text{-}IC}$ allele. Mice carrying the *Shh-CRE* knockin allele (27), *R26R* allele (29), or *Rosa*$^{N1\text{-}IC}$ allele (17) were crossed to generate mice hemizygous

for the *R26R* allele, hemizygous for the *Shh-CRE* allele, and hemizygous for *Rosa*$^{N1\text{-}IC}$ allele. Mice were genotyped as described (18, 27, 29, 48). Timed pregnant CD-1 mice were purchased from Charles River Breeding Laboratory (Wilmington, MA). Longwood Medical Area's Institutional Animal Care and Use Committee (IACUC) approved all animal protocols.

Microarray Hybridization and Analysis. RNA was purified from mouse retinal tissue by TRIzol extraction (Gibco, Carlsbad, CA). cDNA was prepared from RNA, amplified, and labeled as described (49). Pairs of labeled probes were hybridized at 42°C overnight on microarrays consisting of a total of 12,350 clones from the Brain Molecular Anatomy Project clone set (kind gift of Bento Soares, University of Iowa, Iowa City, IA) and additional clones from the laboratory (50). Slides were washed (51) before scanning in an Axon GenePix 4000B Scanner (Axon Instruments, Union City, CA). Data were analyzed by using the GenePix software package (Axon Instruments). A listing of the top 50 clones that were up- and down-regulated at E13.5 and P10 in the *Chx10*$^{N1\text{-}IC}$ retinae are included in Tables 4–7, which are published as supporting information on the PNAS web site.

Cell Culture. The retinae from adult mice were dissected in PBS and dissociated with papain (Worthington, Lakewood, NJ). Papain was activated by mixing 40 μl of papain (500 units/ml; Worthington), 40 μl cysteine/EDTA mix (25 mM cysteine/5 mM EDTA, pH $\approx$6–7) and 320 μl of HBSS/Hepes (normal HBSS/10 mM Hepes) and incubated at 37°C for 15–30 min. The dissected retinae were in activated papain for 20–30 min at 37°C. They were then pelleted for 2 min at 200 $\times$ *g*, and the papain was removed. Four hundred microliters of HBSS with DNase I was added, followed by gentle mixing and incubation at room temperature for 3 min. Further dissociation was by gentle trituration with a P1000 pipette 10–15 times. The retinae were then incubated with the DNase I for 5 min at room temperature. One milliliter of HBSS was added, and the mix was centrifuged for 3 min at 200 $\times$ *g*. The cell pellet was resuspended in serum-free medium [1:1 DMEM/F-12 Ham's (Gibco)/B27 Supplement (Gibco)/20 ng/ml EGF (Invitrogen)/20 ng/ml FGF2 (Invitrogen)/8 μg/ml Heparin low molecular weight (Sigma, St. Louis, MO)/20 ng/100 units/ml penicillin/streptomycin (Gibco). For BrdU incorporation, freshly dissected retinae were cultured with medium (45% DMEM/45% F12 medium/10% FCS) containing BrdU for 1 h at 37°C. Labeled cells were detected according to the manufacturer's instructions (Roche, Indianapolis, IN). A total of 2,000–3,000 cells were scored from two independent retinae for each genotype.

ISH and Immunohistochemistry. All tissue sections (20 μm) were prepared after embedding in OCT. For X-Gal staining, retinal tissue was fixed with 1% PFA/0.5% glutaraldehyde (52). Retinae were stained as whole mounts overnight at 37°C. Section ISH were performed on retinal cryosections as described (53). For immunostaining, the following antibodies were used: anti-Chx10 (rabbit polyclonal, 1:500; C. M. Chen and C.L.C., unpublished results), anti-Pax6 (mouse monoclonal, 1:500; University of Iowa Developmental Studies Hybridoma Bank, deposited by Atsushi Kawakami), anti-glutamine synthetase (mouse monoclonal, 1:200; PharMingen, San Diego, CA), anti-β tubulin (mouse monoclonal, 1:200; Upstate Biotechnology, Lake Placid, NY), anti-GFP (mouse monoclonal and rabbit polyclonal, both 1:500; Molecular Probes, Eugene, OR), and goat anti-mouse or -rabbit Cy3 or Cy5 (1:200; Jackson ImmunoResearch, West Grove, PA). Cells were counterstained with DAPI. Fluorescent images were taken on an Axioplan 2 microscope with a LSM 510 Meta module for confocal imaging. All light microscopy images images were taken on a Nikon (Florham Park, NJ) Eclipse E1000 using a Leica (Deerfield, IL) DC200 camera.

GenBank Accession Numbers. GenBank accession nos. are as follows: *clusterin*, BE996359; *Notch1*, BE981557; *fibroblast growth factor 15* (*FGF15*), BE952015; *secreted frizzled-related protein 2*, *Sfrp2*, BF463274; *deiodinase*, *iodothyronine type III*, *antisense* (*Dio3as*), BE951547; *cyclin D1*, AI850048.

We thank Charlie Murtaugh and Douglas Melton (Harvard University, Boston, MA) for the *Rosa*$^{N1\text{-}IC}$ mice; Paul Scherz, Brian Harfe, and Cliff Tabin for *Shh-CRE* mice; Sheldon Rowan, Douglas Kim, and Takahiko Matsuda for support and technical assistance; and members of the Cepko, Tabin, and Dymecki laboratory for helpful discussions and advice. This work was supported by funds from National Institutes of Health Grant EYO 9676. A.P.J. was supported by National Institutes of Health Grant T32EY007110, and C.L.C. is an Investigator of the Howard Hughes Medical Institute.

1. Cepko CL, Austin CP, Yang X, Alexiades M, Ezzeddine D (1996) *Proc Natl Acad Sci USA* 93:589–595.
2. Edlund T, Jessell TM (1999) *Cell* 96:211–224.
3. Artavanis-Tsakonas S, Rand MD, Lake RJ (1999) *Science* 284:770–776.
4. Furukawa T, Mukherjee S, Bao ZZ, Morrow EM, Cepko CL (2000) *Neuron* 26:383–394.
5. Gaiano N, Nye JS, Fishell G (2000) *Neuron* 26:395–404.
6. Morrison SJ, Perez SE, Qiao Z, Verdi JM, Hicks C, Weinmaster G, Anderson DJ (2000) *Cell* 101:499–510.
7. Hitoshi S, Alexson T, Tropepe V, Donoviel D, Elia AJ, Nye JS, Conlon RA, Mak TW, Bernstein A, van der Kooy D (2002) *Genes Dev* 16:846–858.
8. Jadhav AP, Mason HA, Cepko CL (2006) *Development (Cambridge, UK)* 133:913–923.
9. Yaron O, Farhy C, Marquardt T, Applebury M, Ashery-Padan R (2006) *Development (Cambridge, UK)* 133:1367–1378.
10. Harris WA (1997) *Curr Opin Genet Dev* 7:651–658.
11. Livesey FJ, Cepko CL (2001) *Nat Rev Neurosci* 2:109–118.
12. Dorsky RI, Rapaport DH, Harris WA (1995) *Neuron* 14:487–496.
13. Bao ZZ, Cepko CL (1997) *J Neurosci* 17:1425–1434.
14. Lindsell CE, Boulter J, diSibio G, Gossler A, Weinmaster G (1996) *Mol Cell Neurosci* 8:14–27.
15. Austin CP, Feldman DE, Ida JA, Jr, Cepko CL (1995) *Development (Cambridge, UK)* 121:3637–3650.
16. Scheer N, Groth A, Hans S, Campos-Ortega JA (2001) *Development (Cambridge, UK)* 128:1099–1107.
17. Murtaugh LC, Stanger BZ, Kwan KM, Melton DA (2003) *Proc Natl Acad Sci USA* 100:14920–14925.
18. Rowan S, Cepko CL (2004) *Dev Biol* 271:388–402.
19. Satow T, Bae SK, Inoue T, Inoue C, Miyoshi G, Tomita K, Bessho Y, Hashimoto N, Kageyama R (2001) *J Neurosci* 21:1265–1273.
20. Blackshaw S, Harpavat S, Trimarchi J, Cai L, Huang H, Kuo WP, Weber G, Lee K, Fraioli RE, Cho SH, *et al.* (2004) *PLoS Biol* 2:E247.
21. Linser P, Moscona AA (1981) *Proc Natl Acad Sci USA* 78:7190–7194.
22. Sicinski P, Donaher JL, Parker SB, Li T, Fazeli A, Gardner H, Haslam SZ, Bronson RT, Elledge SJ, Weinberg RA (1995) *Cell* 82:621–630.
23. Walther C, Gruss P (1991) *Development (Cambridge, UK)* 113:1435–1449.
24. Krebs LT, Deftos ML, Bevan MJ, Gridley T (2001) *Dev Biol* 238:110–119.
25. Tropepe V, Coles BL, Chiasson BJ, Horsford DJ, Elia AJ, McInnes RR, van der Kooy D (2000) *Science* 287:2032–2036.
26. Coles BL, Angenieux B, Inoue T, Del Rio-Tsonis K, Spence JR, McInnes RR, Arsenijevic Y, van der Kooy D (2004) *Proc Natl Acad Sci USA* 101:15772–15777.
27. Harfe BD, Scherz PJ, Nissim S, Tian H, McMahon AP, Tabin CJ (2004) *Cell* 118:517–528.
28. Wallace VA, Raff MC (1999) *Development (Cambridge, UK)* 126:2901–2909.
29. Soriano P (1999) *Nat Genet* 21:70–71.
30. Turner DL, Snyder EY, Cepko CL (1990) *Neuron* 4:833–845.
31. Das AV, Mallya KB, Zhao X, Ahmad F, Bhattacharya S, Thoreson WB, Hegde GV, Ahmad I (2006) *Dev Biol* 299:283–302.
32. Fekete DM, Perez-Miguelsanz J, Ryder EF, Cepko CL (1994) *Dev Biol* 166:666–682.
33. Mizutani K, Saito T (2005) *Development (Cambridge, UK)* 132:1295–1304.
34. Grosskortenhaus R, Pearson BJ, Marusich A, Doe CQ (2005) *Dev Cell* 8:193–202.
35. Coffman CR, Skoglund P, Harris WA, Kintner CR (1993) *Cell* 73:659–671.
36. Harris WA, Hartenstein V (1991) *Neuron* 6:499–515.
37. Dyer MA, Cepko CL (2001) *J Comp Neurol* 429:601–614.
38. Marquardt T, Ashery-Padan R, Andrejewski N, Scardigli R, Guillemot F, Gruss P (2001) *Cell* 105:43–55.
39. Wang SW, Kim BS, Ding K, Wang H, Sun D, Johnson RL, Klein WH, Gan L (2001) *Genes Dev* 15:24–29.
40. Brown NL, Patel S, Brzezinski J, Glaser T (2001) *Development (Cambridge, UK)* 128:2497–2508.
41. Fischer AJ, Reh TA (2001) *Nat Neurosci* 4:247–252.
42. Ooto S, Akagi T, Kageyama R, Akita J, Mandai M, Honda Y, Takahashi M (2004) *Proc Natl Acad Sci USA* 101:13654–13659.
43. Kubo F, Takeichi M, Nakagawa S (2005) *Development (Cambridge, UK)* 132:2759–2770.
44. Kubo F, Takeichi M, Nakagawa S (2003) *Development (Cambridge, UK)* 130:587–598.
45. Alvarez-Buylla A, Garcia-Verdugo JM, Tramontin AD (2001) *Nat Rev Neurosci* 2:287–293.
46. Merkle FT, Tramontin AD, Garcia-Verdugo JM, Alvarez-Buylla A (2004) *Proc Natl Acad Sci USA* 101:17528–17532.
47. Doetsch F, Caille I, Lim DA, Garcia-Verdugo JM, Alvarez-Buylla A (1999) *Cell* 97:703–716.
48. Radtke F, Wilson A, Stark G, Bauer M, van Meerwijk J, MacDonald HR, Aguet M (1999) *Immunity* 10:547–558.
49. Tietjen I, Rihel JM, Cao Y, Koentges G, Zakhary L, Dulac C (2003) *Neuron* 38:161–175.
50. Livesey FJ, Young TL, Cepko CL (2004) *Proc Natl Acad Sci USA* 101:1374–1379.
51. Young TL, Cepko CL (2004) *Neuron* 41:867–879.
52. Kwan CT, Tsang SL, Krumlauf R, Sham MH (2001) *Dev Biol* 232:176–190.
53. Chen CM, Cepko CL (2000) *Mech Dev* 90:293–297.